ASTER 스테레오 영상의 폐색영역 보정에 의한 DEM 생성*

이진덕[1※] · 박진성[2]

Generation of DEM by Correcting Blockage Areas on ASTER Stereo Images*

Jin-Duk LEE[1※] · Jin-Sung PARK[2]

요 약

NASA의 Terra 위성에 탑재된 ASTER는 기선고도비 0.6, 15m 해상도의 along-track 디지털 스테레오 영상자료를 제공한다. 43㎞×50㎞ 지역에 대한 ASTER 스테레오영상으로부터 ENVI 4.1 소프트웨어의 자동 스테레오 상관처리과정을 실행하여 15m×15m의 DEM을 추출하였다. ASTER DEM의 정확도를 1:25,000축척의 수치지형도로부터 얻은 DEM을 기준으로 하여 분석한 결과, 높이에서 RMSE ±7~±20m를 나타냈다. RMSE ±10m를 초과하게 하는 요인들로서 구름지역, 수역, 건물지역들을 제외한 지역들의 DEM 정확도는 5.789m의 RMSE를 나타냈다.

따라서 본 연구에서는 구름지역과 그림자 지역을 토지피복 분류에 의해 검출하여 추출된 ASRER DEM(엄밀히 말해서 DSM) 상에서 그 부분들을 제거한 다음, 밴드간 연산기법을 이용하여 이 부분을 수치지형도로부터 추출한 DEM으로 대치함으로써 지형정보의 정확도를 높이고자 하였다.

주요어 : ASTER, 스테레오영상, 수치고도모형, 정확도, 밴드간 연산

ABSTRACT

The Advanced Spaceborne Thermal Emission and Reflection Radiometer (ASTER) on-board the NASA's Terra spacecraft provides along-track digital stereo image data at 15m resolution with a base-height ratio 0.6. Automated stereocorrelation procedure was implemented using the ENVI 4.1 software to derive DEMs with 15m×15m in 43㎞ long and 50㎞ wide area using the ASTER stereo images. The accuracy of DEMs was analyzed in comparison with those which were obtained from digital topographic maps of 1:25,000 scale. Results indicate that RMSE in elevation between ±7 and ±20m could be achieved. Excluding cloud, water and building areas

2010년 1월 16일 접수 Received on January 16, 2010 / 2010년 3월 15일 수정 Revised on March 15, 2010 / 2010년 3월 17일 심사완료 Accepted on March 17, 2010

* 본 연구는 2008 XXIth Congress Society for Photogrammetry and Remote Sensing(2008. 7)에서 발표한 논문을 수정·보완한 것입니다.

1 금오공과대학교 토목환경공학부 School of Civil and Environmental Engineering, Kumoh National Institute of Technology
2 한국아이엠유(주), IMU Korea Ltd
※ 연락저자 E-mail : jdlee@kumoh.ac.kr

as the factors which make RMSE value exceeding 10m, the accuracy of DEMs showed RMSE of ±5.789m.

Therefore for the purpose of elevating accuracy of topographic information, we intended to detect the cloud areas and shadow areas by a landcover classification method, remove those areas on the ASTER DEM and then replace with those areas detached from the cartographic DEM by band math.

KEYWORDS : ASTER, Stereo Images, DEM, Accuracy, Band Math

INTRODUCTION

Generally DEMs have been produced from digital topographic maps, aerial photos and satellite image data and lately DEMs not exceeding one meter are obtained from LiDAR. A DEM is the basic topographic analysis data which are used to represent a contour map, a slope map, a relief map and so on in 3 dimensions and so play an important tool for national land planning, communication, tourism, environment, game industry, defense, etc. Professionals in an array of industries use DEMs to increase their analysis capabilities: target authentication, field communication and data orthorectifcation in defense, volume extraction measurement in mining/exploration, visual representations for presentation, water runoff analysis in civil GIS and so forth.

Digital photogrammetric techniques have been known for decades, but the possibility of using stereoscopic images from satellites for global digital elevation data production did not arise until the launch of the SPOT series in 1986. Today several satellites also offer the possibility for stereoscopic acquisition: MOMS, IRS, KOMPSAT-2, AVNIR, TERRA, IKONOS-2, QUICKBIRD-2, SPOT-5, EROS-A1 and ORBVIEW-3.

ASTER(Advanced Spaceborne Thermal Emission and Reflection Radiometer) is an imaging instrument that is flying on Terra, a satellite launched in December, 1999 as part of NASA's Earth Observing System (EOS). Accounts of ASTER stereo imagery being employed for sensor orientation and DEM extraction are given in several studies. Those studies reported on an evaluation of the geopositioning accuracy and DEM generation and validation from ASTER data using commercial software packages (Cuartero *et. al.,* 2004, Kamp *et. al.,* 2003).

Clouds and shadows on satellite images obstructive to extract various information from the earth's surface like land cover classification. Several techniques have been presented for masking out the clouds. Ackerman *et. al.*(1998) described a physics-based cloud mask algorithm developed for the MODIS instrument using MODIS Airborne Simulator. Their automated routine masks pixels that contain optically thick aerosol, clouds, or shadow. Brumby *et. al.*(2001) compared several techniques for automatically masking out clouds, and will present results for a genetic algorithm approach (using a software package called GENIE) which attempts to evolve a cloud mask achieving automation, robustness, and good classification performance.

In this paper, we will discuss the method of DEM generation from ASTER stereo image data using ENVI 4.1 software. The accuracy of ASTER DEM will be validated by comparing with the reference DEM produced from digital topographic maps at a 1:25,000 scale. When people usually intend to extract topographic information from satellite imagery of a certain area in specified time, cloud areas and shadow areas which are included in some images generally make them be in trouble. In this research we intended to suggest the alternative to overcome this problem and improve the accuracy of topographic information. We focussed to detect the cloud areas and shadow areas by a landcover classification method, remove those areas on the ASTER DEM, strictly speaking, which is called DSM(digital surface model), and then replace with those areas detached from the digital topographic map DEM by band math. Consideration is also given to the utility of the ASTER DEM for mapping application

STUDY AREA AND USED DATA

The test area is a 43㎞×50㎞ rectangle in the province of Gyeongsangbukdo (Southeast of the Korean Peninsula), which has various topographic characteristics including mountainous districts, rivers, built-up districts, flatland and so forth.

The ASTER sensor provides image data in 14 visible, near infrared, short wavelength infrared and thermal infrared spectral bands. Stereo image data are recorded only in Band 3, which is the near-infrared wavelength region from 0.78~0.86μm, using both nadir and aft-looking telescope. From the nominal Terra altitude of 705 km, the "pushbroom" linear array sensor covers 60km-wide ground track at a 15m spatial resolution. As shown in FIGURE 2, there is an approximately 60 sec interval between the time the nadir telescope passes over a ground location and the aft telescope records the same location on the ground track of the satellite. Images generated from the nadir and aft telescopes yield a B/H ratio of 0.6, which is close to ideal for generating DEMs by automated techniques for a variety of terrain conditions.

A major advantages of the along-track mode of data acquisition (as compared to cross-track) is that the images forming the stereo pairs are acquired a few seconds (rather than days) apart under uniform environmental and lighting conditions, resulting in stereopairs of consistent quality that are well suited for DEM generation by automated stereocorrelation techniques (Hirano, 2003,

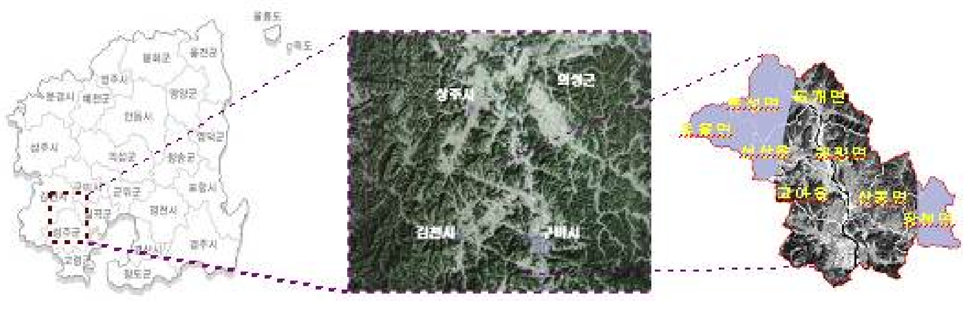

FIGURE 1. Study area

Fujisada, 1994).

The ASTER images used for this study are level 1B data which are acquired on 29th of May, 2004. The stereo pair of the near-infrared backward and nadir images (3N and 3B) was used in the sensor orientation and DEM generation (FIGURE 2). These images have a size of 4200×4100 pixels with a spatial resolution of 15m and scale of 1:1,500,000.

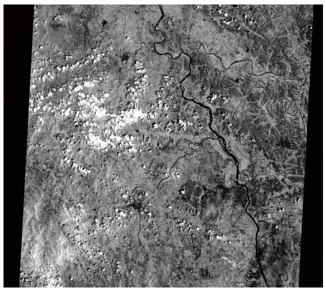

(a) VNIR 3N band

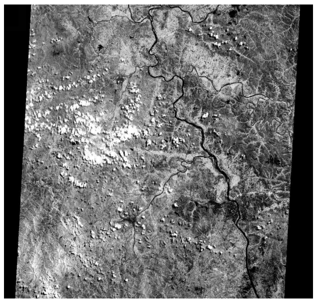

(b) VNIR 3B band

FIGURE 2. ASTER image data of test area

DEM EXTRACTION

The procedure for extracting topographic information from ASTER stereo imagery is showed in FIGURE 3. The mathematical model which forms the basis of the photogrammetric solutions was adopted in the ENVI 4.1 software package. RPC coefficients of the images and 51 conjugate tie points, which are collected in both images 3N and

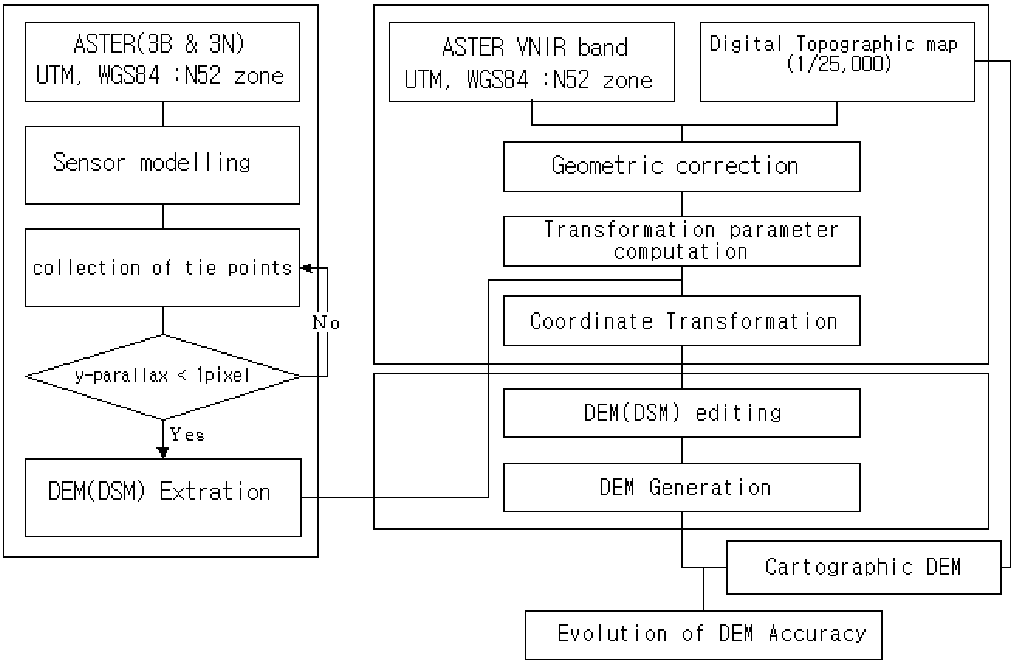

FIGURE 3. The procedure for extracting DEM from ASTER stereo imagery

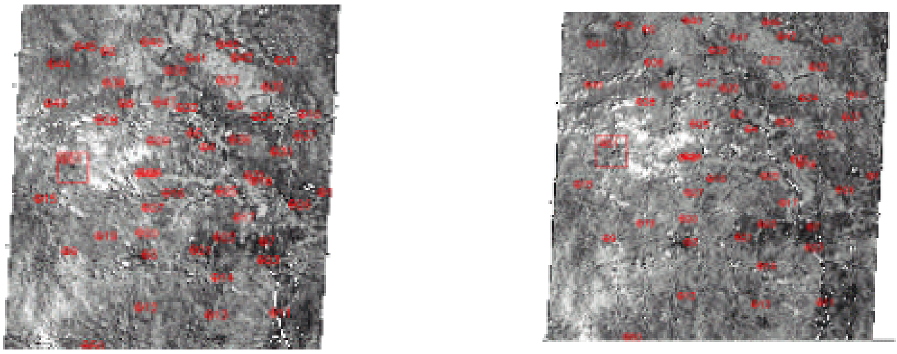

(a) VNIR 3N (b) VNIR 3B

FIGURE 4. ASTER stereo pair with 51 tie points locations

3B, were used for DEM extraction and as a result, image matching was performed with y parallax value of 0.8065. Stereocorrelation has become a standard method of generating DEMs from digital stereo images. Stereocorrelation is a computational and statistical procedure utilized to derive a DEM from a stereo pair of registered images. The core of stereocorrelation is automatic image matching.

FIGURE 4 shows 3N and 3B of the stereo pair with the location of total 51 tie points. Using generated Epipolar images, DEM (digital surface model) was acquired in UTM coordinate system based on the WGS84 ellipsoid (FIGURE 5).

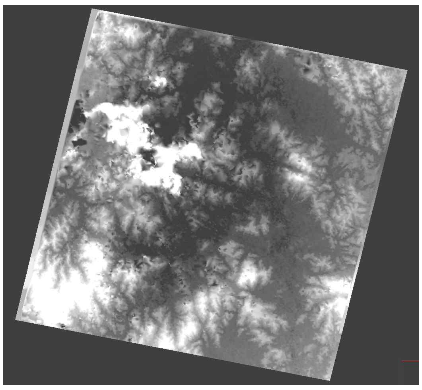

FIGURE 5. Generated DEM

The generated DEM was changed into TM coordinate system which has Eastern Map Origin at Lon 129°00′00″, Lat 38°00′00″ using transformation parameters between ASTER images and digital topographic maps. The image registration for obtaining transformation parameters employed 30 GCPs which were collected in twenty five digital topographic maps with 1:25,000 scale and the accuracy of geometric correction was 0.809 pixel RMSE. 5×5 low pass was used for the interpolation of DEM.

COMBINATION OF CARTOGRAPHIC DEM FOR CORRECTION OF ASTER DEM

1. Land Cover Classification

We needed to supplement DEM of portions hiden by clouds and shadows on the images. A landcover map was produced by maximum likelihood method of supervised classification to detect cloud regions and their shadow regions from the images(FIGURE 6). The area of Gumi city of ASTER image was cut out using 1:25000 scaled digital topographic maps and then band images excluding thermal infrared band were used for classification.

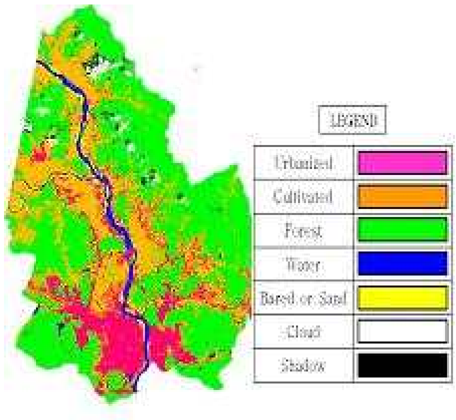

FIGURE 6. The result of supervised classification

TABLE 1. The result of supervised classification

Landcover	Number of pixels	Area (㎢)	Ratio (%)
Cultural	539,843	121.46	27.76
Build-up	274,818	61.83	14.13
Water	60,115	13.53	3.09
Sandy	37,013	8.33	1.90
Mountain	975,421	219.47	50.16
Cloudy	39,669	8.93	2.04
Shadow	17,689	3.98	0.91
Total	1,944,568	437.53	100

2. Band Math for DEM Correction

Masking maps of binary images were derived by applying thresholding to the landcover mask map for clouds and their shadows for the purpose of removing only cloud and shadow areas in the ASTER DEM or detaching only cloud areas and shadow areas in cartographic DEM by band math (multiplication).

The left mask binary image of FIGURE 7 shows the area covered with clouds and shadows were given as the black area of 0 value and the rest area given as the white area of 1 value. This mask image is for removing clouds and their shadows areas from the ASTER DEM. Through Band multiplication, the cloud areas and their shadow areas were removed on the ASTER DEM.

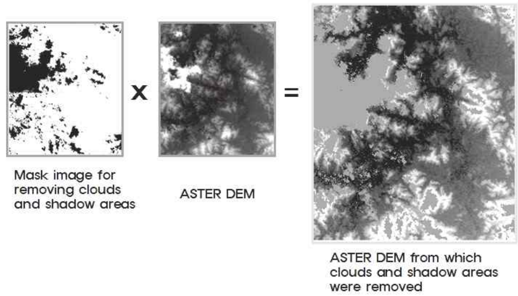

FIGURE 7. Band math(1)

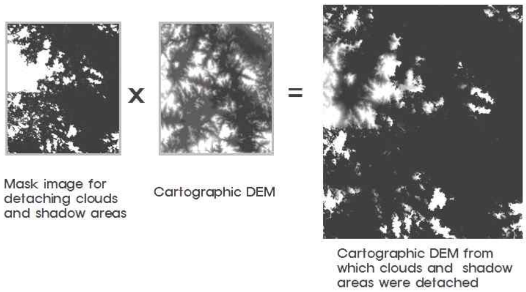

FIGURE 8. Band math(2)

In contrast with FIGURE 7, the left mask image of FIGURE 8 is for detaching clouds and their shadows areas from the cartographic DEM. The binary image shows that cloud and shadow areas were given as the white area of 1 value and the rest area given as the black area of 0 value. Through Band multiplication, the cloud areas and their shadow areas were detached on the cartographic DEM.

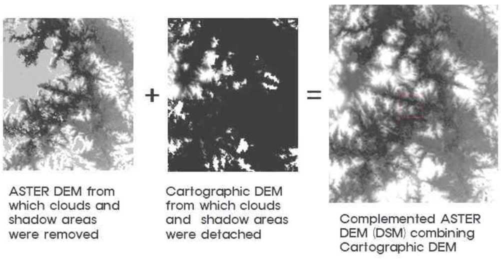

FIGURE 9. Band math(3)

And then the cloud areas and cloud shadow areas removed on the ASTER DEM were replaced with those areas detached on the cartographic DEM by band addition as shown in FIGURE 9.

ASSESSMENT OF ASTER DEM ACCURACY

The DEM extracted from 1:25,000 digital topographic maps was considered as reference data for accuracy assessment. Six transect lines were drawn longitudinally and latitudinally with as shown in FIGURE 10 to compare between ASTER DEMs and reference DEMs.

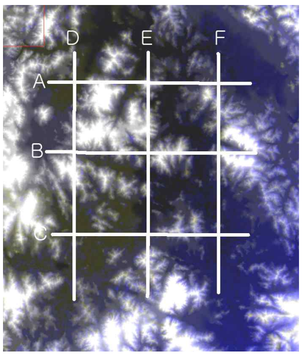

FIGURE 10. Six transects drawn for comparing between ASTER DEM and cartographic DEM

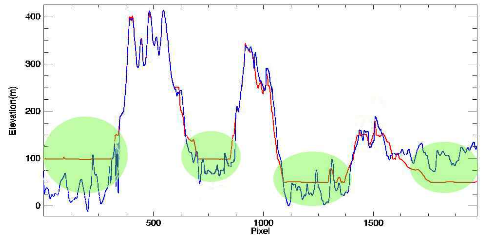

(a) Transect A

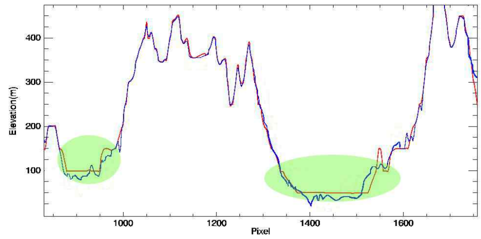

(b) Transect B

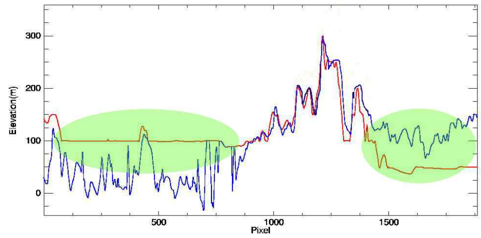

(c) Transect C

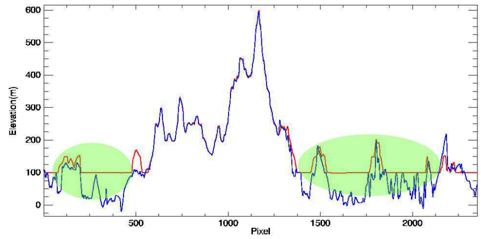

(d) Transect

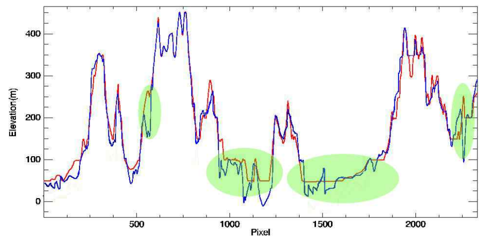

(e) Transect E

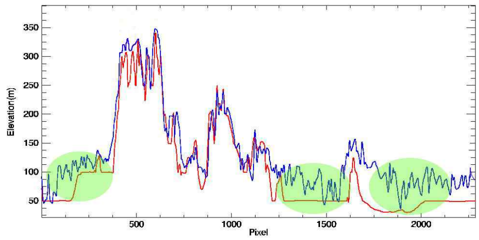

(f) Transect F

FIGURE 11. Profile comparisons between ASTER DEM elevations and reference DEM

In FIGURE 11, ASTER DEMs, which were generated with ENVI software package using stereocorrelation techniques, were plotted against the DEMs extracted from 1:25,000 scale topographic map, yielding an RMSE-z of ±1.14m. The portions depicted with a ellipse in FIGURE 11 show the effects of cloud, water and building-close areas upon big difference between both DEMs. The maximum elevation difference in each transect of (a)~(f) are appeared respectively as 105m, 25m, 120m, 100m, 50m and 100m. On the whole, evaluations of vertical accuracy of ASTER DEM indicate that RMSE of ±7~20m can be expected when using software such as ENVI 4.1.

However since this is about overall area including cloud, water and building-close areas, it is necessary to be analyzed about only the sections not exceeding 10m in each transect. The result showed respectively 5.036m, 3.362m, 6.198m, 3.571m, 7.921m, and 8.648m in RMSE-z along (a)~(f) transect lines. Overall accuracy within the limits of the difference of 10m is ±5.789m.

The 3D data recovered by photogrammetric techniques can be imported in GIS environment for further analysis and visualization. Vector and raster data describing the topography, landcover and landuse of the terrain can be overlaid on the DEM in order to obtain 3D combined model. The incorporation of elevation and terrain data can improve the information extraction for example, in discriminating wetlands, flood mapping, and forest management. Different GIS applications with the recovered ASTER DEM have been reported (Chrysoulakis *et. al.,* 2004)

DISCUSSION AND CONCLUSION

On the whole, the evaluation of vertical accuracy of ASTER DEM indicates that RMSE-z of ±7~20m can be expected. Excluding cloud, water and building-close areas, that is regions exceeding 10m in each transect, it is shown that RMSE-z values are 5.036m, 3.362m, 6.198m, 3.571m, 7.921m, and 8.648m respectively in the transect lines of (A)~(F). Overall accuracy within the limits of the difference of 10m is ±5.789m.

To recover DEMs of parts hidden by the cloud areas and cloud shadow areas on the ASTER DEM, the DEMs of object areas detached from cartographic could be applied by thresholding and band math.

The results obtained in this study shows that ASTER stereo images are suitable for a range of environmental mapping tasks involving the use of DEMs. The 3D data recovered by photogrammetric techniques can be imported in GIS environment for further analysis and visualization. The potentials of middle resolution satellite images for the generation of DEM and its use in GIS has been verified using the ASTER on board the NASA's satellite Terra. The ASTER scenes, available at very low price (55$ each), represent a convenient and reliable data for the DEM generation and land analysis between 1:25,000 and 1:50,000 scale when it is assumed that cloud, shadow, water and building-close areas are excluded or replaced with cartographic DEM. ASTER data were also proved to be suitable for topographic mapping of high relief areas at a scale of 1/50,000 and less with contour intervals of 20m or larger.

ACKNOWLEDGEMENTS

This research was supported in 2008 by Research Fund, Kumoh National Institute of Technology. KAGIS

REFERENCES

Ackerman, S.A., Strabala, K.I., Menzel, W.P., Frey, R.A., Moeller, C.C., Gumley, L.E. 1998. Discriminating clear sky from clouds with MODIS. Journal. Geophysical. Research Vol. 103:32141 - 32158.

Brumby, S.P., Hirsch, K.L., Davis, A.B. Harvey, N.R., Rohde, C.A. 2001. Genetic Refinement of Cloud-Masking Algorithms for the Multi-Spectral Thermal Imager (MTI). IEEE, 1152-1154. web site http://rcc.lanl.gov/content/isis/green/publications/davis IGARSS2001.pdf.

Cuartero, A., Felicisimo, A.M., Ariza, F.J. 2004. Accuracy of DEM Generation from Terra-ASTER Stereo Data. IAPRS&SIS, Vol. 35, Part B6, pp.225-260.

Chrysoulakis, N., Abrams, M., Feidas, H., Velianitis, D. 2004, Analysis of ASTER Multispectral Stereo Imagery to Produce DEM and Land Cover Databases for Greek Islands: The REALDEMS Project. In: Prastacos, P., Cortes, U. De Leon, J. L., Murillo, M. (Eds): Proceedings of e-Environment: Progress and Challege, 411 - 424pp.

Fujisada, H. 1994. Overview of ASTER Instrument on EOS-AM1 Platform, Proceedings of SPIE, The International Society for Optical Engineering, Vol.2268:14-36.

Hirano, A., Welch, R., Lang, H. 2003. Mapping from ASTER Stereo Image Data: DEM Validation and Accuracy Assessment, Journal of Photogrammetry & Remote Sensing. ISPRS, 57:356-370.

Kamp, U., Bolch T., Olsenholler, J. 2003. DEM Generation from ASTER Satellite Data for Geomorphometric Analysis of Cerro Sillajhuay, Chile/Bolivia, Annual Conference Proceedings, ASPRS, Anchorage, Alaska. KAGIS